Composites Science and Technology 150 (2017) 102–110

Contents lists available at ScienceDirect

Composites Science and Technology

journal homepage: http://www.elsevier.com/locate/compscitech

Characterization of residual stress and deformation in additively manufactured ABS polymer and composite specimens

Wei Zhang [a, b, c], Amanda S. Wu [d], Jessica Sun [c], Zhenzhen Quan [a], Bohong Gu [a], Baozhong Sun [a, **], Chase Cotton [e], Dirk Heider [c], Tsu-Wei Chou [b, c, *]

[a] College of Textiles, Donghua University, Shanghai 201620, PR China
[b] Department of Mechanical Engineering, University of Delaware, Newark, DE 19716, USA
[c] Center for Composite Materials, University of Delaware, Newark, DE 19716, USA
[d] Materials Engineering Division, Lawrence Livermore National Laboratory, CA 94550, USA
[e] Department of Electrical and Computer Engineering, University of Delaware, Newark, DE 19716, USA

ARTICLE INFO

Article history:
Received 16 May 2017
Received in revised form
13 July 2017
Accepted 16 July 2017
Available online 17 July 2017

Keywords:
Residual stress
Shrinkage
Microstructure
Processing parameters
Additive manufacturing

ABSTRACT

Residual stresses induced in the layer-by-layer fabrication process of additively manufactured parts have significant impact on their mechanical properties and dimensional accuracy. This work aims to characterize the residual stress and deformation in specimens based on unreinforced acrylonitrile-butadiene-styrene (ABS), carbon nanotube reinforced ABS and short carbon fiber reinforced ABS. The shrinkage and displacement fields were obtained, respectively, by thermal treatment as well as Digital Image Correlation observation of specimens before and after sectioning. The microstructure and porosity of additively manufactured specimens were also examined using X-ray micro-computed tomography. Specimen shrinkage and porosity content were significantly influenced by the process parameters of raster angle and printing speed, as well as material types. Faster printing speed led to larger porosity and residual stress, as well as higher shrinkage after specimen thermal treatment. Raster angle had a greater influence on specimen shrinkage and porosity as comparing to printing speed. Composite printing wires based on carbon nanotube and short carbon fiber in ABS greatly reduced specimen shrinkage and deformation, while increased the porosity, especially for carbon fiber reinforced ABS specimens.

1. Introduction

Additive manufacturing is defined as a "process of joining materials to make parts from 3D model data, usually layer upon layer, as opposed to subtractive manufacturing and formative manufacturing methodologies" [1] by ISO/ASTM. It refers to a family of fabrication methodologies including fused deposition modeling (FDM) [2], stereo lithography (SLA) [3], selective laser sintering (SLS) and selective laser melting (SLM) [4], inkjet modeling (IJM) [5] and others [6]. In recent years, additive manufacturing has evolved rapidly and been widely used in various manufacturing fields such as aerospace [7], automobile [8], biomedical [9], building [10] and many others [11–13]. This tremendous success could be attributed mainly to its outstanding ability to directly manufacture complex parts without special tools, to greatly reduce material waste, and to significantly reduce the time and cost of manufacturing for novel products and small-quantity productions [14–18].

The effects of an array of processing parameters, such as raster angle, printing speed, layer thickness, etc. on the mechanical properties of additively manufactured parts have been well documented in the literature [19–23]. In order to improve the performance of additively manufactured parts and broaden their applications, researchers have explored various types of printing materials, such as polymers, nanocomposites, fiber reinforced composites, etc. [24–31]. Another important aspect relevant to the mechanical performance of additively manufactured parts is repeated heating and cooling [32,33] resulting from the layer-by-layer building process. Significant residual stresses [34] can thus exist in additively manufactured part. Apart from their detrimental influence on mechanical performance, residual stresses could give rise to part distortion and dimensional inaccuracy [35–38]. Some

---

[*] Corresponding author. Department of Mechanical Engineering, University of Delaware, Newark, DE 19716, USA.
[**] Corresponding author.
E-mail addresses: sunbz@dhu.edu.cn (B. Sun), chou@udel.edu (T.-W. Chou).

http://dx.doi.org/10.1016/j.compscitech.2017.07.017
0266-3538/© 2017 Elsevier Ltd. All rights reserved.

efforts have been made by researchers in identifying residual stresses in additively manufactured parts. For example, Karalekas and Rapti [39]. used epoxy based photopolymer to study the processing dependence of SLA solidification residual stress using the hole-drilling strain gage method of stress relaxation. Karalekas and Aggelopoulos [40] investigated the shrinkage strains in a SLA cured acrylic photopolymer resin. Kantaros et al. [41] studied the residual strains in ABS parts fabricated by FDM using fiber Bragg grating method. Casavola et al. [42] measured the residual stress in FDM parts made of ABS employing the hole-drilling method combined with electronic speckle pattern interferometry. These research efforts have greatly facilitated the understanding of residual stresses in additively manufactured parts. However, more studies with respect to characterization techniques, printing materials and processing parameters still need to be conducted to minimize the detrimental effects of residual stress.

This work aims to characterize the residual stress and deformation in additively manufactured specimens based on unreinforced ABS, carbon nanotube reinforced ABS and carbon fiber reinforced ABS. The shrinkages and displacement fields were obtained by thermal treatment as well as Digital Image Correlation combined with sectioning of specimens, respectively. The effects of two key processing parameters, namely, raster angle and printing speed, as well as reinforcement materials, including carbon nanotube and carbon fiber, on specimen properties have been characterized. The microstructure and porosity of additively manufactured specimens were also examined using X-ray micro-computed tomography.

2. Experiment

2.1. Specimen preparation

In this work, fused deposition modeling was adopted to fabricate additively manufactured specimens. A total of 27 types of specimens have been fabricated using a QIDI Tech dual-nozzle 3D printer (Ruan Qidi Technology Co., Ltd., Ruan, Zhejiang, China). Three kinds of materials, including pure ABS wire, carbon nanotube reinforced ABS wire (CNTABS) and short carbon fiber reinforced ABS wire (CFABS) (3DTECH, USA) were used. The carbon nanotube content in the wire was measured to be around 8 wt% via thermogravimetric analysis (TGA) in the nitrogen gas, as shown in Fig. 1. The significant weight loss of the samples reflected the thermal decomposition of the ABS matrix. The short carbon fiber content was around 15 wt% [16]. The length distribution of short carbon fibers in the wire was also given in Ref. [16]. The carbon fiber lengths varied from 5 μm to 465 μm, with a number-based average of 71.5 μm. In the fabrication process, three raster angles of 0°, ±45°and 0°/90° as well as three printing speeds of 40 mm/s, 60 mm/s and 80 mm/s were selected to build the specimen in the horizontal plane (X-Y). The raster angle indicates the direction of wire printing with respect to the longitudinal X-axis of the specimens, as shown in Fig. 2. The other processing parameters are shown in Table 1. Two kinds of specimen sizes of around 75 × 20 × 3 mm and 40 × 15 × 3 mm were fabricated to study the shrinkage and displacement fields, respectively. There are 12–13 layers each specimen.

2.2. Shrinkage measurement

In order to measure the shrinkage of additively manufactured specimens, thermal treatment was carried out with the heating temperature of 180 °C and heating time of 1 h. The dimensions in length, width and height of specimens before and after thermal treatment were measured by a Vernier caliper with the reading resolution of 0.01 mm. The shrinkage of an additively manufactured specimen in a specific direction was calculated as follows:

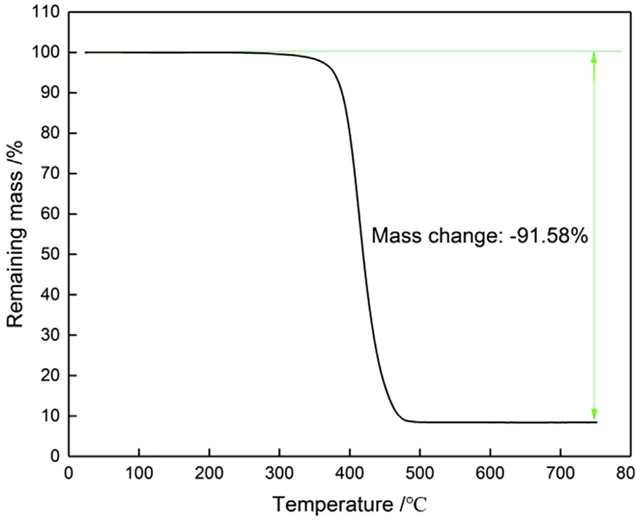

Fig. 1. TGA plot of the as-received CNTABS wire under temperature range of the 25–750 °C.

Shrinkage (%) = ((original dimension (mm.) - dimension after thermal treatment (mm.)) / original dimension (mm.)) × 100%

2.3. Surface displacement field measurement

In an effort to characterize specimen residual stress induced by the additive manufacturing process, surface displacement fields were measured by Digital Image Correlation. Digital Image Correlation is a 3D, full-field, non-contact optical technique to measure contour, deformation, vibration and strain on almost any material. In this work, it was employed by digitally comparing images acquired before and after releasing the localized stress by sectioning the specimen. In the measurement, a specimen was painted using a flat white spray paint and a black speckle pattern was manually applied using a flat black spray paint, with a minimum drying time of 24 h at ambient pressure and room temperature in between coatings. After that, the specimen was imaged using a dual camera setup before and after sectioning via lubricated diamond saw. Fig. 3 shows the images of three specimens (ABS, CFABS and CNTABS) before and after painting and sectioning. The displacement fields were calculated using ARAMIS Professional Digital Image Correlation algorithm (GOM International AG) by comparing the acquired images before and after sectioning. The displacement field so obtained is indicative of the surface-level residual stress in the specimen.

2.4. X-ray micro-computed tomography

The SkyScan 1172 X-ray micro-CT system (Bruker Corp., Billerica, Massachusetts, U.S.) was used to characterize the microstructure and void distribution of additively manufactured specimens. In order to save scanning time, specimens were cut to the size of 8 × 20 × 3 mm. X-ray source voltage and current were 40 KV and 250 μA, respectively. The scanning resolution was around 5.4 μm/pixel. The image size was set as 2048 × 1024 pixel. A series of 2D images in X-Z plane were acquired to record the attenuation of X-